ACS Catalysis

Review

pubs.acs.org/acscatalysis

Unraveling the Complexity of Catalytic Reactions via Kinetic Monte Carlo Simulation: Current Status and Frontiers

Michail Stamatakis[†] and Dionisios G. Vlachos*[,‡]

[†]Department of Chemical Engineering, University College London, Torrington Place, London WC1E 7JE, U.K.

[‡]Department of Chemical and Biomolecular Engineering, Center for Catalytic Science and Technology, University of Delaware, 150 Academy Street, Newark, Delaware 19716, United States

Supporting Information

ABSTRACT: Over the past two decades, the necessity for predictive models of chemical kinetics on catalytic surfaces has motivated the development of ab initio kinetic Monte Carlo (KMC) simulation frameworks. These frameworks have been successfully used to investigate chemistries of academic interest and industrial importance, such as CO oxidation, NO oxidation and reduction, ethylene hydrogenation, CO hydrogenation to ethanol, and water-gas shift. These studies have shed light on the effect of catalyst composition, surface structure, lateral interactions, and operating conditions on the apparent turnover frequency of the chemistries of interest. Yet, extending the existing KMC approaches to study large chemistries on complex catalytic structures poses several challenges. In this review, we discuss the recent milestones in the area of KMC simulation of chemical kinetics on catalytic surfaces and review a number of studies that have furthered our fundamental understanding of specific chemistries. In addition, we provide directions for future research aiming toward incorporating detailed physics and chemistry, as well as assessing and improving the accuracy of KMC methods, toward developing quantitative models of surface kinetics.

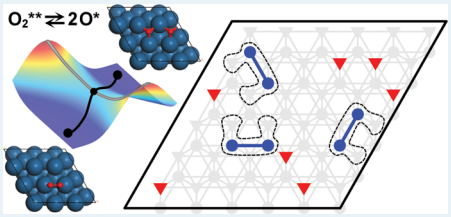

KEYWORDS: *rational catalyst design, kinetic Monte Carlo, surface kinetics, adsorption, desorption, diffusion, reaction, adsorbate−adsorbate interactions, cluster expansion*

INTRODUCTION

Over the past fifteen years, computational methods in catalysis have attracted a widespread interest as means for investigating the underlying pathways of an overall reaction, predicting the apparent turnover frequencies, and providing insights into the design of suitable catalysts.[1−4] The majority of computational work has typically employed density functional theory (DFT) or higher-level methods to estimate the parameters of the elementary steps that compose an overall reaction, and inferences about the rate determining step (RDS) are often made based on energetics alone. Closing the gap between calculations and even the idealized surface science experiments necessitates prediction of reaction rates and species coverages using some kind of averaging of microscopic events on the catalyst. This in turn needs reaction rate theory calculations and the subsequent use of a kinetic model. For the latter task, one can employ Langmuir−Hinshelwood closed form models, order-of-magnitude estimation using Sabatier analysis,[5−7] mean-field microkinetic modeling,[8−10] or detailed kinetic Monte Carlo (KMC) simulation.[11−14] Among these, mean-field microkinetic modeling has dominated over the past decade because of its mathematical simplicity and the smaller number of parameters needed for simulation.

The KMC model is the only one that can resolve events taking place on the catalytic surface at the microscopic level, explicitly accounting for spatial inhomogeneity arising from different types of sites and spatial correlations due to lateral interactions between adsorbates. Even though KMC is computationally the most intensive method among the ones employed for computing reaction rates, it provides the "exact averaging" of microscopic events. With the computational power and the need for predictive models rising, one may expect further development of KMC methods and associated software to enable researchers to close the gap with experiments. To the extent that transition state theory (TST) captures the reaction dynamics for the system of study, the accuracy of the KMC method is limited by that of the DFT method used to parameterize the rate constants and the energetics of the adsorbates, as well as the accuracy of modeling the energetics (approximation of Hamiltonian).

In this perspective, we first review the milestones in the development of KMC approaches for the detailed simulation of kinetics on catalytic surfaces, and subsequently discuss the recent studies that have used first-principles KMC to shed light on specific chemistries. Furthermore, we identify outstanding challenges in the development of KMC frameworks for incorporating detailed physics and chemistry, as well as the assessment and improvement of the accuracy of these frameworks. Finally, we propose directions for future research toward achieving these goals.

Received: August 29, 2012
Revised: October 19, 2012
Published: October 24, 2012

   dx.doi.org/10.1021/cs3005709 | *ACS Catal.* 2012, 2, 2648−2663

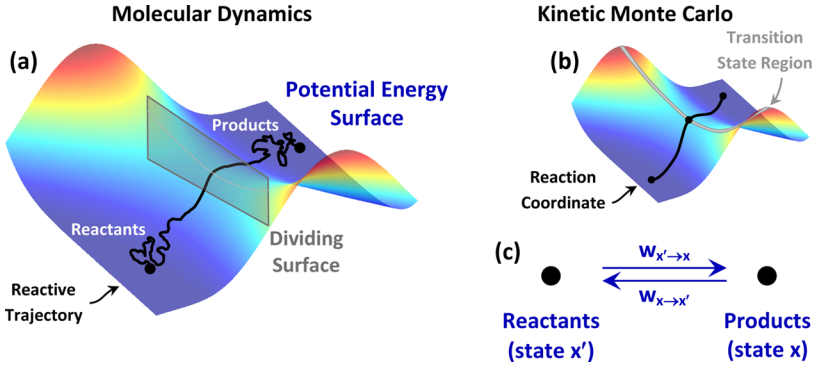

Figure 1. In studying reactions via molecular dynamics, one simulates trajectories on a potential energy surface, and monitors the crossings through a dividing surface separating reactants and products (a). By assuming that the dynamics of the crossing are slow and treat all other processes as quasi-equilibrated, one can employ TST to calculate the reaction rate (b). Subsequently, one can use the KMC approach to simulate reactions as the transition between discrete states, which represent reactant and product configurations (c).

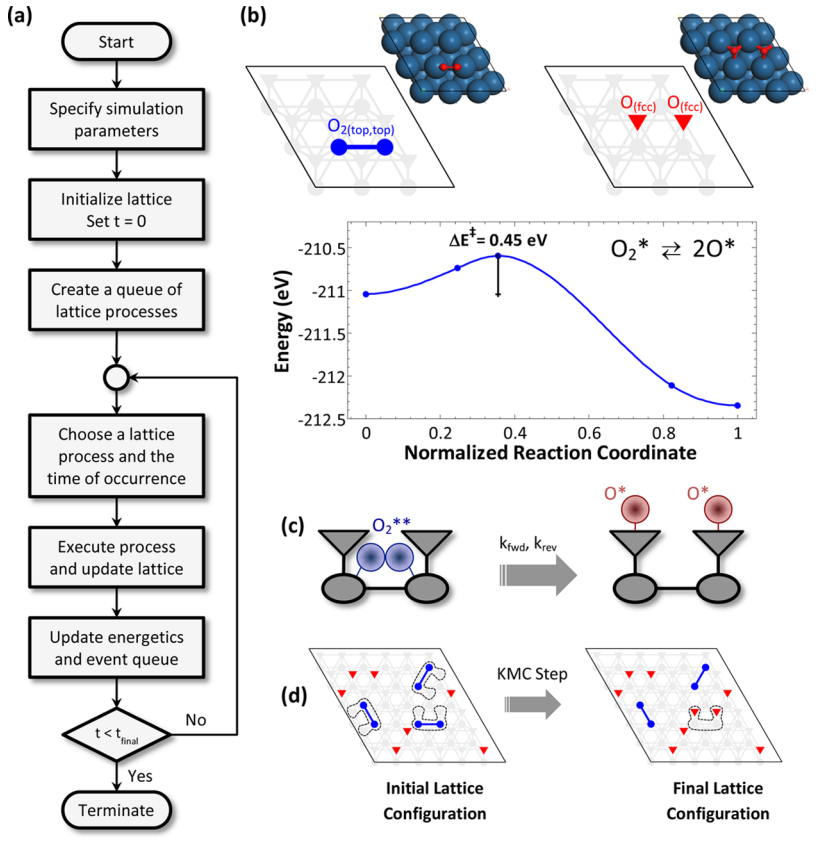

Figure 2. (a) Generic algorithm for a lattice KMC simulation. Initialization entails the definition of a reaction network and the specification of operating conditions. (b, c) Each elementary step can be investigated through DFT codes. An example for the O_2 dissociation on Pt is shown: The top pictures (b) show the unit cell and the configurations used in a DFT code, along with the lattice representation of these configurations, and an NEB calculation showing the MEP whose maximum is the TS. The scheme below (c) portrays a reaction pattern in the KMC framework. The reaction's forward and reverse kinetic constants k_{fwd} and k_{rev} can be calculated through eq 2. (d) During a KMC simulation the reaction pattern is being searched for on the lattice, and each occurrence is listed as a possible lattice process. At the next KMC step, one of these possible processes is executed, and the lattice state is updated.

BACKGROUND ON THE KINETIC MONTE CARLO METHOD

The KMC approach is formally attributed to Bortz et al.[15] and was developed for Ising spin systems; yet, the method is mathematically general. The catalytic surface is represented as a lattice, namely a collection of connected sites that can be of different types, such as top, bridge, fcc hollow and hcp hollow. The elementary events of adsorption, desorption, diffusion and surface (Langmuir−Hinshelwood or Eley−Rideal) reactions, are simulated as instantaneous processes that happen at random times, that is, as a Markov process (a process without memory). This approach is justified by the assumption that these events entail crossings in a potential energy surface (PES) whose time scales are much larger than those of the equilibration inside a potential energy well (Figure 1).[13,16] Upon execution of an elementary event, a change in the state or configuration (spatial

dx.doi.org/10.1021/cs3005709 | ACS Catal. 2012, 2, 2648−2663

snapshot) of the lattice occurs (e.g., an occupied site by CO is being emptied because of desorption).

In a mean field (MF) treatment, the coverage (the fraction of occupied sites by each species) describes the temporal information of each species. A key assumption in the MF treatment is that the system is spatially homogeneous, at least at the mesoscopic length scale (of the order of several nanometers), that is, both catalyst sites and adsorbates are uniformly distributed. The system evolves deterministically, as prescribed via ordinary differential equations. In contrast, in the KMC method, one uses probabilities to describe the various snapshots (lattice states). Specifically, the temporal evolution of the probability $P(\mathbf{x},t)$ of finding the system at a particular configuration $\mathbf{x}$ at time t, is governed by the so-called master equation:

$$\frac{dP(\mathbf{x}, t)}{dt} = \sum_{\mathbf{x}' \neq \mathbf{x}} [w_{\mathbf{x}' \to \mathbf{x}} \cdot P(\mathbf{x}', t) - w_{\mathbf{x} \to \mathbf{x}'} \cdot P(\mathbf{x}, t)] \quad (1)$$

where $w_{\mathbf{x}' \to \mathbf{x}}$ denotes the probability density for a transition from state $\mathbf{x}'$ to state $\mathbf{x}$ in the next dt time interval, because of the occurrence of an elementary event. This parameter $w_{\mathbf{x}' \to \mathbf{x}}$ is essentially a stochastic rate constant, and is often referred to as the propensity of that particular elementary event.

It is typically impossible to solve eq 1 even numerically, because of the extremely large number of possible configurations of the surface. The KMC method simulates trajectories whose statistics are in line with eq 1, according to the pseudoalgorithm outlined in Figure 2a: at first, the lattice is initialized with a random configuration, and an ordered list of all the possible lattice processes that can occur is generated. Subsequently, the algorithm enters a loop, at each step of which a process is randomly executed (in line with the propensity of occurrence thereof), and the lattice state and propensities are updated. The output of a simulation provides the temporal evolution of the lattice, as well as the number of molecules of species arriving at and produced from the surface. By postprocessing these results, one can calculate apparent turnover frequencies (TOFs), coverages, and selectivities. Sensitivity and reaction path analyses can also be performed. For more information on the algorithmic details of KMC and its accelerated versions, the reader is referred to Chatterjee and Vlachos.[17]

MILESTONES IN THE DEVELOPMENT OF KMC METHODS FOR DETAILED SURFACE KINETICS

Early KMC frameworks utilized ad hoc values for the rate constants of elementary events, semiempirical estimation methods (e.g., bond-order conservation (BOC)) of rate constants, simplified reaction networks, and a simplistic picture of the catalyst and the active site, for example, a square or hexagonal lattice representing the (100) or (111) facets.[18−23] Next we discuss key developments of predictive KMC models.

First-Principles KMC. Extension to realistic chemistries is possible using first-principles calculations to obtain rate constants. This requires the coupling of KMC and quantum chemistry methods (Figure 2b-d), out of which DFT is predominantly used because of its low computational cost. DFT solves the Schrödinger equation for the interacting electrons of a molecular structure by mapping it into a noninteracting problem, consisting of the Kohn−Sham equations.[24−26] These equations are *exact*, and contain an effective potential which prescribes the electronic structure of the system. In this description, the total energy of the system consists of the kinetic energy of the electrons, Coulomb interactions, and finally, the exchange-correlation (XC) energy. The latter part is the most difficult to treat, and even though there are several approximations of varying levels of accuracy, currently there is no final theory that yields its exact value.[27−29] We will return to this point later in our discussion.

By invoking the Born−Oppenheimer approximation, one can fix the positions of the nuclei and calculate the total energy of a molecular structure with respect to these positions, thereby obtaining the PES (Figure 1). In practice, one is interested in the minima thereof, which correspond to stable species, and the saddle points, which correspond to the transition states (TSs). Both the aforementioned structures can be identified without having to compute the entire PES, by using geometry optimization methods. Once such a structure has been found, one can subsequently calculate the vibrational frequencies, and the moments of inertia (if applicable), thereby obtaining all information necessary for a statistical mechanical representation of that structure.

As noted earlier, the value of this information for KMC simulations lies in the fact that it can be used to compute rate constants. Thus, for each elementary event, the (thermal) rate constant can be formulated using TST, as follows:[16,30]

$$k_{rxn} = \frac{k_B \cdot T}{h} \cdot \frac{Q^{\ddagger}}{Q_{reac}} \cdot \exp\left(-\frac{\Delta E^{\ddagger}}{k_B \cdot T}\right) \quad (2)$$

where k_B and h denote Boltzmann's and Planck's constants, respectively; T is the temperature; $Q^{\ddagger}$ and Q_{reac} denote the quasi-partition functions (vibrational, translational, and rotational components) of the TS and the reactants, respectively; and $\Delta E^{\ddagger}$ is the zero-point corrected activation energy. In the above expression, both the activation energy $\Delta E^{\ddagger}$ and the partition functions $Q^{\ddagger}$ and Q_{reac} can be obtained from first principles, by calculating the total energies, vibrational frequencies, and moments of inertia of all participating species and TSs. To identify the latter, one can use a variant of the nudged elastic band (NEB) method, which also provides a series of images along the entire minimum energy path (MEP) connecting two minima of the PES, or the dimer method, which requires only two images to converge to the TS.[31−34] More details on how eq 2 is applied to calculate the rates of various elementary steps (adsorption, desorption, diffusion, and Eley−Rideal reactions) are provided in the Supporting Information.

Neurock and co-workers were among the first to couple KMC and DFT methods. The resulting approach is nowadays known as first-principles or ab initio KMC method.[11,12] In this approach, one uses DFT data to a priori construct a database for the activation energies of reaction events and a model for the energetic interactions between adsorbates. The latter model incorporates adsorbate binding on different sites (such as top, bridge, and hollow), and pairwise additivity or BOC to tackle lateral interactions (Figure 3).[35] Thus, in contrast to the ab initio molecular dynamics (MD), whereby the force field is continuously updated quantum mechanically, here the main parametrization of the KMC input is done only once (one way or sequential coupling in the multiscale nomenclature).[36] Fast diffusion is taken into account by equilibrating the lattice after each adsorption, desorption or reaction event. Scheffler and co-workers[13,37] and Jansen and Lukkien[38] developed a similar simulation framework. Moreover, Lukkien and co-workers have established a general purpose on-lattice KMC code, which has

dx.doi.org/10.1021/cs3005709 | ACS Catal. 2012, 2, 2648−2663

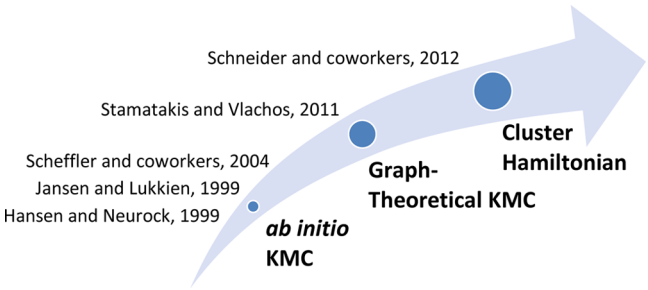

Figure 3. Milestones in the development of recent KMC methods.

been integrated in the Materials Studio software by Accelrys as a module by the name Kinetix.[39]

While in principle straightforward, the a priori KMC/DFT coupling described above is only approximate. Currently, the errors incurred due this approximation are poorly understood, and the lack of predictability often exhibited by DFT methods undermines the accuracy of first-principles KMC.[29] These points are further discussed below.

Graph-Theoretical KMC. To tackle the geometric complexity often encountered in realistic chemistries, Stamatakis and Vlachos recently developed a KMC approach that uses graph theory to represent the elementary events of adsorption, desorption, diffusion, surface and Eley−Rideal reactions (Figure 3).[40−42] This graph-theoretical KMC approach constitutes a general and straightforward framework for the representation of arbitrarily complex lattice chemistries. The latter may contain elementary steps in which multidentate species are encountered in a variety of binding configurations, and participate in elementary events that involve intricate neighboring patterns as predicted via DFT. The high fidelity of this KMC approach comes at a minimal computational expense as compared to the traditional single- and two-site event KMC.[40]

Cluster-Expansion Hamiltonians. The aforementioned KMC frameworks have typically employed relatively simple models for the adlayer energetics, mostly limited to short-ranged pairwise-additive interactions. In spite of their usefulness in qualitative investigations, such models have been shown to be unable to accurately capture the structure of the adlayer and consequently the probability that a reactive configuration occurs on the lattice.[43−46] Moreover, the accuracy of early energetic models based on the Unity Bond Index-Quadratic Exponential Potential (UBI-QEP) approach (such as the BOC models used by Neurock and co-workers)[12,35] has not been assessed thoroughly as discussed by Maestri and Reuter.[47]

To rectify these issues, recent research has focused on the application of comprehensive cluster expansion-type Hamiltonians for the simulation of surface kinetics (Figure 3).[43] These Hamiltonians can incorporate long-ranged, as well as multibody interactions, thereby lifting the limitation to pairwise-additive nearest-neighbor interactions. Moreover, their parametrization is more general and flexible than that of the UBI-QEP energetic models, preventing the appearance of coverage-dependent spurious contributions discussed by Maestri and Reuter.[47]

Cluster expansions have been extensively used for the calculation of thermodynamic quantities and phase diagrams of adsorbate layers.[43,44,48−55] The formulation of such expansions is general and amounts to expressing the energy of the system as a sum of single-, two-, and multibody interactions. For one species and a single site, the Hamiltonian takes the following form:

$$\mathrm{H}(\boldsymbol{\sigma}) = H_0 + \beta\cdot\sum_{i=1}^{N_L}\sigma_{i,k} + \frac{1}{2}\cdot\sum_{i=1}^{N_L}\sum_{\substack{j=1\\ i\neq j}}^{N_L} J_{i,j}\cdot\sigma_i\cdot\sigma_j + \frac{1}{6}\cdot\sum_{i=1}^{N_L}\sum_{\substack{j=1\\ i\neq j}}^{N_L}\sum_{\substack{k=1\\ k\neq i\\ k\neq j}}^{N_L} J_{i,j,k}\cdot\sigma_i\cdot\sigma_j\cdot\sigma_k + \ldots \quad (3)$$

where σ_i is the occupation variable which, following the lattice-gas convention, represents the presence or absence of an adsorbate at site i (σ_i = 1 and 0, respectively). Moreover, H_0 is a constant pertinent to the energy of an unoccupied surface site, β, $J_{i,j}$, $J_{i,j,k}$, and so forth are the energies of the one-body, pairwise, three-body and higher order terms. Parameters β, $J_{i,j}$, $J_{i,j,k}$, and so forth are referred to as effective cluster interactions (ECIs). The factors $^1/_2$, $^1/_6$, and so forth prevent overcounting of a single cluster caused by renumbering the sites involved therein.

Extension to multiple species is straightforward; however, the computational cost of evaluating the Hamiltonian increases with the number of species because of the large number of clusters (patterns) that enter the expansion[48] (more details on this will be discussed later in the Computational Challenges section). Furthermore, more recently, Lerch et al. developed a cluster expansion formulation that can accommodate virtually any number of different site types.[56]

Fitting the ECIs using ab initio calculations is tedious, but there exist computational codes that can perform this process automatically with minimal user input.[57−59] Although a comprehensive KMC framework that incorporates a general cluster expansion formulation is still lacking, several studies have incorporated detailed cluster expansions in simulations of thermal desorption.[60−63] The first study to utilize cluster expansions for catalytic rate estimation was recently carried out by Schneider and co-workers.[64] In this study, a Monte Carlo simulation scheme for equilibrating adlayer structure of atomic oxygen on Pt(111) was coupled with a kinetic model for NO oxidation. This approach establishes the groundwork for future research aiming at the development of predictive models of surface kinetics.

Yet, parametrization of cluster-expansion Hamiltonians is nontrivial. Constructing such energetic models for complex systems comprising numerous species which participate in complex chemistries is computationally very intensive. As a result, only fairly small reaction networks have been studied so far. Another challenge is that the accuracy of the fitted ECIs is limited by the accuracy of the first-principles method used to calculate the total energy for given lattice configurations. For instance, for O adatoms adsorbed on Pd(100), Reuter and co-workers estimate the accuracy of the GGA XC functionals to be around 0.06 eV.[45] Because of such errors, trying to include several higher order (multibody) terms in the cluster expansion will in fact result in overfitting: instead of improving the accuracy, the DFT error will be incorporated in the model Hamiltonian.[46] Improving the accuracy of DFT methods will help overcome this limitation.

REALISTIC CHEMISTRIES STUDIED VIA FIRST-PRINCIPLES-BASED KMC SIMULATION

The KMC method explicitly takes into account surface inhomogeneity, adsorbate localization and spatial correlations, which cannot be captured using the Sabatier analysis or mean-

dx.doi.org/10.1021/cs3005709 | ACS Catal. 2012, 2, 2648−2663

field microkinetic modeling. Moreover, the coupling of KMC with DFT calculations renders the simulation a truly first-principles approach. From an efficiency perspective, KMC can simulate reactions with a computational expense that is much lower than that needed for molecular dynamics. The reason for these savings is that KMC focuses on the coarse time-scale of barrier crossing, instead of simulating entire dynamical trajectories on a PES. Thus, several studies have employed this powerful method to elucidate the catalytic mechanisms for chemistries of practical interest, taking place on metal as well as oxide catalysts. These are briefly discussed next.

CO Oxidation. The CO oxidation chemistry has attracted significant attention over the past decade, since its simplicity enables detailed modeling. It has therefore served as a prototype to test the predictions of first-principles KMC codes. In addition, this chemistry is of environmental importance for removing toxic CO from exhausts.[65]

The CO oxidation on $RuO_2(110)$ has been extensively investigated by Reuter, Scheffler, and co-workers.[13,37,66−68] In those studies, the $RuO_2(110)$ surface was modeled as a lattice with two types of sites, bridge and cus. The adsorption of O_2 (dissociative) and CO, the diffusion of adsorbed CO and atomic oxygen, as well as the CO_2 formation, were analyzed with DFT and the parameters were incorporated into a first-principles KMC framework. The simulation results were in agreement with experimental data for conditions ranging from ultrahigh vacuum (UHV) to industrially relevant pressures,[13,37] and the rate-limiting step was identified by applying a degree of rate control (DRC) analysis.[68]

Moreover, surface inhomogeneity, arising from the location of different site types, was investigated and shown to have a marked effect on shaping the temperature programmed reaction (TPR) spectra.[67] Such an effect is brought about by the spatial correlations between the active sites on the surface and cannot be captured by mean-field models.[66,69] The mean-field model overestimates the range of CO partial pressures for which the catalyst is active and does not accurately identify the gas composition resulting in maximal TOFs.

On the other hand, it has been argued that even a first-principles KMC approach may yield unreliable results, because of the extreme sensitivity of the simulated behavior on the input parameters.[70] Thus, in a recent study, Over and co-workers critically assessed the simulation results obtained for CO oxidation on $RuO_2(110)$ using three different parameter sets,[37,71,72] in view of the uncertainty of the energetic parameters entering the kinetic rate expressions.[70] It was found that small variations in the activation energies can result in markedly different physics; in particular, both the most frequent elementary step as well as the most abundant reaction intermediate (MARI) may change. On the basis of these observations, it was argued that it is necessary to validate KMC models using detailed experimental techniques that can probe surface composition, as well as comparing experimental and simulated rates over an extended range of temperatures. This uncertainty in the predictions of kinetic models goes well beyond the KMC method (is equally applicable to mean field models as well), and underscores the need for rigorous uncertainty quantification methods[73] especially at low temperatures (activity) and for processes with competing reaction pathways (selectivity).

The CO oxidation reaction has also been modeled on metal catalysts, in particular Pt, Rh, and Pd single crystal surfaces[74−78] and Au nanoclusters.[42] Völkening and Wintterlin[78] presented kinetic Monte Carlo simulations of this reaction on Pt(111). The "basic model" simulated therein utilized parameter values obtained from experimental data and assumed a single site type, but failed to capture the experiments. This model was subsequently extended to incorporate coordination-dependent reactivity, thereby being able to reproduce experimental observations, in particular, the reaction order of 1/2 with respect to oxygen coverage, the shapes of the domains occupied by adsorbed CO and O, as well as the higher reactivity of the domain boundaries. However, a more detailed variant, taking into account reactive interstitial CO molecules on the (2×2)O phase, overestimates the reaction order. Petrova and Yakovkin[77] also studied this system, suggesting a model for CO oxidation in which oxygen is the active species, and showing good agreement with TPR experiments. In that study, lateral interactions between CO−CO and CO−O and O−O were modeled with effective potentials, the parameters of which were adjusted according to experimental data on adlayer stability. Nagasaka et al.[74] performed KMC simulations of this reaction on Pt(111), incorporating lateral interactions between adsorbates as determined by DFT calculations. Their model of the adlayer energetics assumes pairwise additivity and accounts for multiple adsorbates and site types, in particular, O on fcc sites, and CO on bridge and top sites. The simulations were found to reproduce the experimentally observed behavior, in particular the coverages at various temperatures and pressures, the adlayer structures, and the sites thereof where the reaction takes place.

Furthermore, Rogal et al.[75] studied the CO oxidation chemistry on Pd(100) and showed that a surface oxide structure can be stable at ambient pressures, under which the surface can be catalytically active. They postulated that at steady state, transitions between the reduced and the oxidic Pd(100) structure may take place. In a detailed study, Liu and Evans[76] used KMC simulation in a multiscale modeling context, to simulate the CO oxidation on Rh(100) and Pd(100). The simulations were found to be in good agreement with experimentally obtained TPR spectra, and provided insight into the onset of propagating reaction fronts at mesoscale.

Finally, Stamatakis et al.[42] recently investigated the reaction rates and poisoning effects for the CO chemistry on MgO-supported Au_6 nanoclusters. Depending on the type of support defects, Au_6 was found in different charge states: Mg-vacancies result in positively charged Au_6, and no defects in neutrally charged Au_6. Both Au_6^+ and Au_6^0 were found to exhibit low CO-binding energies and be inactive toward CO oxidation. Au_6^- clusters, resulting from O-vacancies on the support, can transiently convert CO, but eventually get poisoned by carbonate. This study underscored the importance of the cluster's charge state and provided a possible explanation of the experimentally observed inactivity of Au_6.

NO Reduction and Oxidation. NO-related chemistries have also served as prototypes for the assessment of KMC modeling techniques, and are of practical significance because of environmental and health impacts. Thus, several studies have investigated such chemistries using empirical KMC models focusing on the impact of geometry for clusters of sites catalyzing the NO reduction by CO,[79−81] the effect of impurities blocking catalytic sites[82] as well as the effect of step sites[83] in this system, the adsorbate-induced phase transition and the oscillatory characteristics of NO reduction by NH_3,[84] as well as the different pathways and the effect of lateral interactions of NO decomposition during TPR experiments.[85,86] Further, kinetic oscillations, reaction fronts, and pattern formation phenomena

dx.doi.org/10.1021/cs3005709 | ACS Catal. 2012, 2, 2648−2663

for the NO chemistries have received much attention, and have been simulated with deterministic models[87−92] as well as KMC methods.[93−99]

The studies just mentioned employed estimated kinetic parameters, often deduced from experiments. Hansen and Neurock[35] were the first to use DFT calculations and the BOC method coupled with KMC simulation to investigate NO reduction on Rh(100). The authors elucidated the interplay between NO dissociation and desorption for different coverages in the presence of strong repulsive interactions between the adsorbed species, and showed that the model is in good agreement with experimental TPR data. More recently, Mei et al.[100] performed detailed simulations that demonstrated the interplay between the NO oxidation and reduction chemistries on the (100) and (111) facets of Pt nanoparticles. It was thus found that NO oxidation to NO_2 can take place on both facets, although it is much more favored on the (111) facet. NO reduction to N_2 occurs exclusively on the (100) facets. However, structural sensitivity effects were not observed for either chemistry, since the fractions of (100) over the (111) number of sites are approximately constant for the sizes of particles investigated. These results are in agreement with the experimentally observed structural insensitivity of NO oxidation.

There have also been efforts to elucidate the details of the adlayer energetics. Van Bavel et al.[101] focused on the effect of lateral interactions between the NO, O, and N species participating in NO dissociation. By comparing the DFT interaction energies with those obtained by fitting KMC-calculated TPR spectra to experiments, they showed that DFT calculations overestimate repulsion: for instance, the N−N nearest-neighbor interaction energy was found equal to 58 kJ/mol by DFT calculations, but a value of only 33 kJ/mol was obtained by fitting the KMC model to experiments. For O-NO nearest-neighbors, the interaction energy was calculated to be 31 kJ/mol using DFT and 21 kJ/mol from KMC fitting.[101] It was thus concluded that DFT can only provide a qualitative picture of the underlying physics. In that study, only pairwise interactions between nearest and next-nearest neighbors were considered, and as the authors note, more detailed studies should address the assumption of pairwise additivity. In fact, recent studies by Schneider and co-workers have shown that this assumption is likely to give an oversimplified description of the adlayer energetics.[43,64] More specifically, by performing a detailed analysis of cluster expansions for the oxygen−oxygen lateral interactions, it was found that for an accurate description of the energetics, one needs to include up to eighth nearest neighbor pair-repulsions, as well as two triplets (three-body terms).[43] These energetic models were incorporated into a kinetic model of NO oxidation on Pt(111) and were shown to be in marked agreement with experimental data.

Hydrogenation and Decomposition of Alkenes and Alkynes. *Ethylene Hydrogenation.* The hydrogenation of ethylene is a prototype system of hydrogenation reactions, and is important in the conversion of olefins into higher-octane gasoline blending components. An early KMC study of this reaction on Pt focused on diffusion, activation of surface intermediates, and steric hindrance effects.[102]

Hansen and Neurock developed a first-principles KMC model of ethylene hydrogenation on Pd(100), which utilized DFT calculated energetics at the zero coverage limit, whereas adsorbate lateral interaction effects were incorporated within the BOC framework.[12,103] Their model predicts an apparent reaction order which is negative with respect to ethylene and less than unity with respect to hydrogen, in agreement with experimental data. These results were attributed to the repulsive lateral interactions, the competition in the adsorption sites, as well as the different size of the ethylene molecule and the hydrogen atom. This work was later extended by Neurock and co-workers,[104,105] to study Pd(111) as well as bimetallic Pd/Au(111) surfaces. It was found that higher surface Au compositions result in a strengthening of the metal−hydrogen and metal−carbon bonds, thereby promoting the hydrogenation activity, but also in a weaker binding of H_2 on the surface, which hinders the catalytic activity. Compensation between these two effects leads to alloying Au with Pd having an overall negligible effect of on the activity, consistent with experiments.[104,105]

Acetylene Hydrogenation. As an extension to the aforementioned studies, Mei et al. also investigated the selective hydrogenation of acetylene on Pd(111) and showed that the reaction proceeds via a vinyl intermediate.[106] The simulated apparent activation energies and reaction orders obtained with the first-principles KMC simulation method were in good agreement with experimental results. The inclusion of lateral interactions in the model was found to have only a minimal effect on the calculated overall activation energy. Yet, interactions were shown to have a marked effect on surface coverages and intrinsic reaction rates, and were deemed necessary for accurately calculating selectivity and reaction orders.[106] More recently, Mei et al. simulated the hydrogenation of ethylene/acetylene mixtures on Pd and Pd−Ag alloys, showing that alloying decreases the overall rate, but significantly increases the selectivity toward ethylene hydrogenation.[107]

Ethylene Conversion to Ethylidyne. In a recent study, Mei, Rösch and co-workers investigated the pathways for ethylene conversion to ethylidyne on Pd(111) and Pt(111), using first-principles KMC simulations.[108] The approach taken was similar to that by Neurock and co-workers where DFT calculations are employed to construct a first-principles kinetic database and lateral interactions are modeled using the semiempirical BOC approach.[12,103] It was shown that ethylene conversion to ethylidyne proceeds though a sequence of two dehydrogenation steps, yielding vinyl and subsequently vinylidene, which subsequently gets converted to ethylidyne (Figure 4). The latter

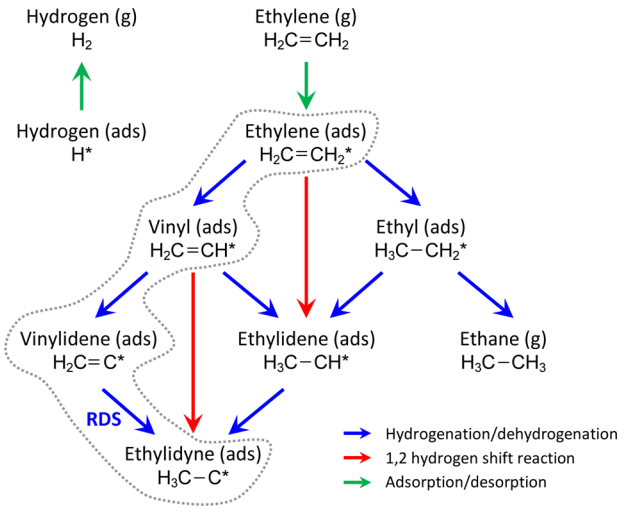

Figure 4. Pathways in the conversion of ethylene to ethylidyne. Highlighted inside the dotted curve is the predominant pathway, with RDS marking the rate determining step. Redrawn from ref 108 (Aleksandrov et al.).

dx.doi.org/10.1021/cs3005709 | ACS Catal. 2012, 2, 2648−2663

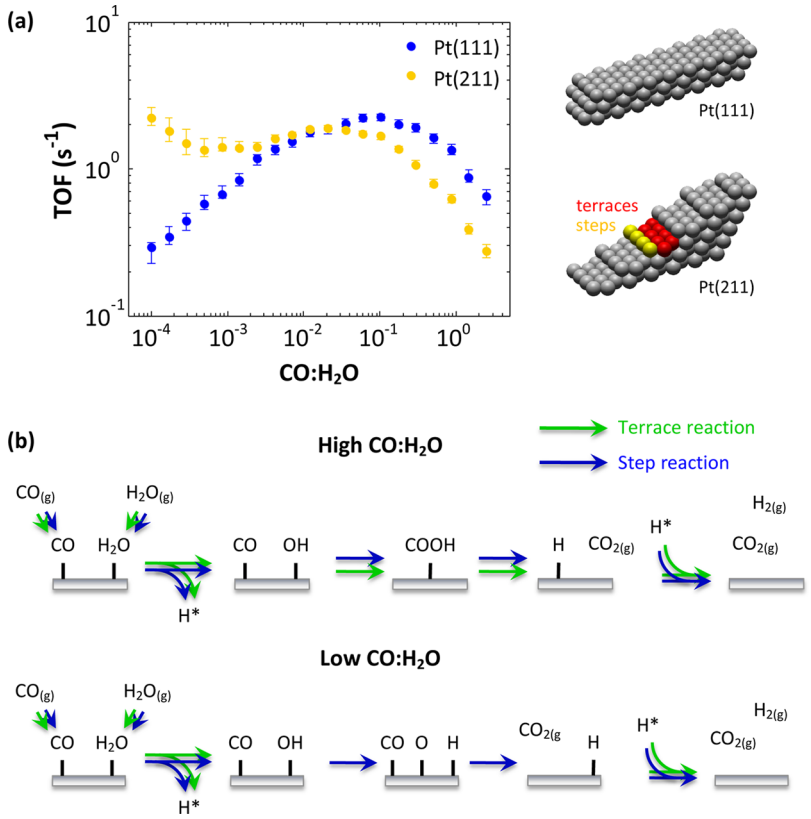

Figure 5. (a) Variable reaction sensitivity for the water-gas shift reaction on single crystal Pt surfaces: for high $CO:H_2O$ ratios, Pt(111) and Pt(211) exhibit similar activities (negligible structure sensitivity). For low $CO:H_2O$ ratios, the stepped surface exhibits a much higher activity. (b) For high $CO:H_2O$ ratios, the carboxyl pathway on both terraces and steps is dominant. For low $CO:H_2O$ ratios, water splitting is observed at the step sites, followed by CO oxidation and CO_2 and H_2 desorption.

reaction (vinylidene hydrogenation to ethylidyne) was found to be the RDS. It is important to note that hydrogenation reactions were found to exhibit lower barriers than dehydrogenations; yet, the low coverages of adsorbed hydrogen on the surface result in the vinylidene hydrogenation being the RDS. Similar behavior is seen in oxidative dehydrogenation of polyols.[109] This is a general and often overlooked finding, whereby the rate of bimolecular reactions is often very low compared to unimolecular reactions, despite favorable energetics, because of low coverages of one of the coreactants (an intermediate). This result underscores the importance of kinetic simulations (mean-field or KMC) in gaining a fundamental understanding of catalytic processes.

Water-Gas Shift. The water-gas shift (WGS) reaction constitutes a more complicated system, which can be thought of as an intermediate between the aforementioned model chemistries and large-scale reaction mechanisms. WGS is employed for removing CO from mixtures of CO and H_2,[110] and has recently attracted attention as a means of producing H_2 downstream of biomass conversion processes.[111] A variety of transition metals have been investigated as potential catalysts for this process, among others Cu and Pt.[10,112,113]

Aiming at investigating structure sensitivity effects for this reaction on Pt, Vlachos and co-workers used the graph-theoretical KMC simulation framework[40] coupled with DFT calculations. The latter yielded the energetics for the elementary steps of the WGS mechanism occurring at combinations of step and terrace sites, which were subsequently used in simulating the WGS reaction on single crystal Pt surfaces with different step site densities.[41] The KMC simulations revealed that for industrially relevant conditions ($CO:H_2O > 1$), the WGS reaction exhibits minor structure sensitivity, with the steps and the terraces both contributing to the overall activity (Figure 5a). This result agrees with the experimental finding that the turnover frequency for this reaction is independent of particle size.[114] On the contrary, for low $CO:H_2O$ ratios, the steps exhibit much higher activity than the terraces (Figure 5a).

This difference in the structure sensitivity at low versus high $CO:H_2O$ ratios was rationalized on the basis of changes in the dominant reaction pathway (Figure 5b). In particular, for high $CO:H_2O$ ratios (CO-rich feeds), the reaction proceeds through the carboxyl pathway at both step and terrace sites. On the other hand, for low $CO:H_2O$ ratios (CO-lean feeds), water decomposition to atomic H and O is observed at step sites, followed by direct CO oxidation and CO_2 and H_2 desorption therefrom.

Identification of the active site has been a long-standing goal of catalysis, and is often assumed that steps are the most active sites. Yet, these simulations point to an obvious conclusion, that is, steps often bind species more strongly and may get poisoned easier than terraces. Thus, it is not obvious which site contributes to activity and selectivity for different chemistries and operating conditions. This study provided the first evidence that the active site may depend on operating conditions and entail multiple sites (a nonlinear average of activity at steps and terraces), in contrast to the preconceived notion of a single active site. In addition, the dominant chemistry (e.g., MARI, RDS) may change with type of active site. Given the ability of resolving detailed structure and shape and the need to capture "communication" or coupling between sites via multisite reactions or surface diffusion (which is absent from mean-field models), it may be expected that KMC

dx.doi.org/10.1021/cs3005709 | ACS Catal. 2012, 2, 2648−2663

simulations will become commonplace in future studies addressing structure sensitivity of catalytic reactions.

Chemistries Involving Oxygenated Hydrocarbons. In view of recent research on biomass conversion to fuels and chemicals, fundamental investigations of the pathways and kinetics of chemistries that involve oxygenated hydrocarbons are timely. Despite the immense chemical complexity of biomass conversion processes, theoretical methods can be used to obtain insight into specific chemistries, which can then be integrated as modules in an overall reaction mechanism. Herein, we review studies that have used first-principles KMC methods for such chemistries.

Acetic Acid Decomposition. Hansen and Neurock investigated the decomposition of acetic acid during TPR on Pd(111) using a first-principles KMC model[115] that was able to reproduce the salient features of the experiments.[116,117] The simulations revealed the formation of oxygen adatoms at low temperatures, subsequently giving rise to water, consistent with experiments. The simulations were also able to explain the three TPR peaks in the absence of preadsorbed oxygen, in terms of the low temperature desorption of acetic acid (1st peak), the hydrogenation of acetate (2nd peak) and the decomposition of acetate (3rd peak). This last peak occurs in tandem with CO_2 evolution because of acetate decarboxylation.

Partial Oxidation of Methanol. Methanol has been suggested as an energy carrier alternative to hydrogen, and is already being utilized as a fuel in the direct methanol fuel cell technology.[118] Motivated by these potential applications, Groß and co-workers studied the partial oxidation of methanol on oxygen-covered Cu(110).[119] KMC simulations that employed DFT-derived barriers were unable to predict several experimental observations, such as the water desorption at low temperatures (250 K), the formaldehyde formation around 350 K, and the high H_2 peak around 360 K.[120] Satisfactory agreement between experiments and simulations was achieved only after adjusting the barriers of all but one of the elementary steps considered in the mechanism. The discrepancies observed were attributed to DFT error, the low accuracy of the lateral interactions model (the only interactions included were between H and methoxy), as well as the assumption of a homogeneous surface that neglects defect sites.

Ethanol Synthesis from Syngas. Conversion of synthesis gas to ethanol is pertinent to fuel and chemical production from renewable feedstocks, such as biomass and shale gas, and from coal. Mei et al.[121] recently investigated the performance of Rh-based/SiO_2 catalysts in ethanol production from syngas using first-principles KMC simulations and experiments. The effect of different promoters was investigated and the Rh/Mn/SiO_2 catalyst was found to be thermodynamically stable and exhibit improved selectivity toward ethanol production. The activities and selectivities calculated from KMC simulations were in qualitative agreement with experiments and shed light on the engineering of catalysts with optimal performance.

Lessons Learned. Several reactions have been studied over the past few years with the ab initio KMC method. One of the important outcomes of the studies just reviewed is that with the advent of first-principles KMC simulation, one is now capable of studying realistic chemistries theoretically, and explaining how microscopic processes at the nanoscale give rise to the observable catalytic properties of a material. The value of this framework lies in multiple unique characteristics: first, the spatial information taken explicitly into account by KMC allows for detailed investigation of the effect of geometric structure of catalyst (nanoparticle size and shape), the nature of the active site, multiple active sites (e.g., support, perimeter and metal sites), and the spatial arrangement of and communication between active sites. All these aspects cannot be modeled correctly with mean-field models. Moreover, the temporal component of KMC simulation allows for the calculation of reaction rates, which are impossible to calculate using (equilibrium) grand-canonical MC simulations, and computationally intractable using molecular dynamics. Finally and most importantly, the coupling of KMC with ab initio calculations makes the predictions of such a framework relevant to chemistries of practical interest, a feature that was lacking in early studies that focused on prototype systems.

First-principles KMC methodologies can thus be used to obtain a complete "profile" of a catalytic reaction mechanism, as they yield an abundance of information including surface coverages and most abundant species, turnover frequencies, selectivities, TPD and TPR spectra, reaction path analysis, the RDS, and 2D topological maps of activity and selectivity. This information can be used in combination with experimental data to validate or refute hypotheses about a mechanism or the active site(s), improve the performance of known catalysts, or even engineer materials with better catalytic properties. For instance, a general lesson learned through KMC simulation is that the lowest barrier pathway is not necessarily the preferred one, because of certain species' low coverages. The latter can at times be interrogated experimentally through operando techniques. Another broad conclusion that emerged from KMC studies is that the active site is not necessarily unique, but may entail multiple catalytic sites and change as a function of operating conditions. Experiments performed on different catalytic structures under various conditions have and will continue to enrich our understanding on such structure-sensitivity effects.

CURRENT CHALLENGES IN THE DEVELOPMENT OF ACCURATE KMC SIMULATION

Clearly, first-principles KMC constitutes a powerful and versatile multiscale modeling framework that can offer valuable insight into catalytic phenomena. Nevertheless, there are still major challenges in the development of accurate KMC methods with predictive power. These challenges may pertain to the inadequate description of the underlying physics and chemistry, as well as to the computational cost arising from the inefficiency of the simulation.

Physics/Chemistry Challenges. "Physics/chemistry challenges" relate to how realistic the simulated processes are and whether the list of elementary events is complete. The latter issue can also be thought of as a computational challenge. Moreover, there is always the "materials-gap" problem originating from the fact that real catalytic structures are far from the idealized single-crystal surfaces typically considered in periodic DFT calculations. For instance, the presence of defects, even in single-crystal surfaces, is not accounted for in a KMC model, because defects are hard to characterize experimentally. In the present discussion, however, we focus on the fact that first principles KMC models are subject to the error of the ab initio method used to identify the elementary steps, and may altogether be missing physics that become important, or even dominate system behavior, under certain conditions.

Limitations in the Predictability of DFT Methods. In principle, it is possible to couple KMC simulation with high-level ab initio methods; yet, in practice DFT is the preferred option because of its computational efficiency. While being an

dx.doi.org/10.1021/cs3005709 | ACS Catal. 2012, 2, 2648−2663

indispensable tool in computational catalysis and materials science, the accuracy of a particular DFT implementation depends on the type of basis set used and the approximation of the XC functional employed. With regard to the latter, the so-called "Jacob's ladder" orders the approximate functionals with increasing accuracy.[29,122]

DFT methods have been shown to exhibit errors that can result in quantitative and qualitative deviations from experimental observations. In particular, from a quantitative perspective, semilocal density functionals usually overestimate surface stability, but at the same time predict higher chemisorption energies (overbinding).[123,124] From a qualitative perspective, there have been cases where the site preference predicted by DFT for even simple adsorbates is not in agreement with experiments. A notorious example is the "CO-puzzle", in which DFT methods predict that CO on Pt(111) binds at the 3-fold fcc site, whereas experimental results show that the most stable binding configuration is on an atop site followed by a bridge site.[125−127]

Such inaccuracies undermine the predictability of ab initio KMC. For instance Van Bavel et al.[101] demonstrated deviations between TPR spectra for the NO dissociation on Rh(100): since the repulsions between N, O, and NO were overestimated by DFT, N* was found to leave the surface much too quickly (at about 100 K lower temperatures than the experiment) for high initial NO coverages. It actually turns out that even small errors in the energetics calculated by DFT may result in large errors in the rate constants because of the exponential dependence of the Arrhenius eq 2. This point is further discussed later as a computational challenge ("Sensitivity Analysis and Uncertainty Quantification" section). Moreover, predicting the binding site incorrectly could introduce artificial steric effects and competitive adsorption dynamics between different adsorbates. For instance, in the case of CO oxidation on Pt(111), the DFT prediction that CO binds to the fcc site would introduce a competition with O adatoms for this site.

Clearly, DFT is not yet at the stage that it can be treated as a fully predictive tool. However, ongoing research efforts in the DFT community are dedicated to the development of better and more computationally efficient approximations.[29] In the short term, the energetics calculated by DFT codes have to be cautiously accepted and corroborated by experimental evidence before being incorporated into KMC, or their effect on the predictions of KMC should be carefully assessed.

Heat and Mass Transfer Effects. In the majority of KMC simulations of catalytic surfaces, it is implicitly assumed that the surface is thermally equilibrated, and that the gas-phase concentrations are uniform. While this approximation may be suitable for small-scale systems with no diffusional limitations, it does not address the pellet and reactor scales. The assumptions of uniform temperature and concentration may be violated under realistic conditions. For instance, thermal equilibration may be unattainable for a very exothermic reaction that releases rapidly thermal energy at the nanoscale followed by slow dissipation in the adlayer and the bulk phase of the catalyst. Moreover, highly active catalytic surfaces would give rise to gradients in the gas-phase concentrations close to the interface, rendering the uniform gas-phase assumption inadequate.

The mathematical foundations of such coupled multiscale models have been developed more than a decade ago, for example refs 36, 128, and 129. Recent studies aiming at incorporating these effects have been carried out by Matera and Reuter[130,131] as well as Mei and Lin,[132] who developed hybrid models combining continuous computational fluid dynamics (CFD) with first-principles KMC. While these studies address heat transfer effects at the macroscale, the problem of local release of thermal energy and dissipation thereof at the microscale may render such frameworks inadequate. Moreover, the use of continuous models for describing mass transfer in systems involving small pores could result in errors if the mean free path is larger than the pore diameter (breakdown of the continuum approximation). Finally, hybrid models often suffer from numerical instability, because of the coupling of different length scales, which results in passing incorrect noise from the KMC to the CFD model.[133]

Resolving these issues necessitates the development of novel frameworks that are capable to seamlessly incorporate heat and mass transfer effects for realistic CFD calculations. In particular, the release and (slow) dissipation of thermal energy at the microscale is fundamentally linked with the assumption that the dynamics in all degrees of freedom except the motion along a reaction coordinate are in equilibrium. Reaction rate theory formulations that relax this assumption by incorporating friction (Kramer's theory) would allow one to compute accurate kinetic rate constants to use as input to KMC.[16] Dissipation to the bulk phase of the catalyst could be taken into account by coupling the dynamics of the adsorbates with the phonons of the catalytic material.

Moreover, tackling the mass transport problem at the microscale could be achieved by coupling the on-lattice master equation for the surface with the reaction-diffusion master equation for the gas-phase (also known as the multivariate master equation).[134−137] A KMC scheme for the latter essentially employs a stochastic counterpart of the finite volume method.[138] The seamless coupling between these two stochastic microscopic models would provide a numerically more robust way to treat mass transport than that of hybrid models. An alternative for simulating the gas-phase near the catalyst is to use the direct simulation Monte Carlo (DSMC) method of Bird for rarified flows.[139] For supported catalysts, the specific gas-phase simulation platform depends on the pore size of the support.

Catalyst Dynamics: Reconstruction, Sintering, and Mixing of Bimetallics. KMC simulations of catalytic phenomena often consider a fixed lattice and neglect the dynamical restructuring of the surface, which can alter the catalytic properties.[140] For instance, such reconstructions have been known to induce hysteresis, excitability, and pattern formation for CO oxidation on Pt surfaces.[141,142] Patterns, such as spiral waves,[141] are notable examples of complexity, and challenge the traditional view of a catalytic surface being a static "template".

A limited number of KMC studies have focused on reconstruction effects. Monine et al.[143,144] have developed hybrid models for the reconstruction of the Pt(110) surface in the CO oxidation. The KMC submodel simulates the elementary events of the reconstruction using barriers obtained through DFT calculations and experiments, whereas the adsorption, desorption, and reaction dynamics are treated via a mean-field model. More recently, Noussiou and Provata presented a CO oxidation model on Pt(100),[145] which incorporates reconstruction by switching between a rectangular and a hexagonal lattice structure, but employs a very simple (the Ziff-Gulari-Barshad prototype) reaction model.[19] The criterion for switching between the two lattice configurations is related to the CO coverage: if the coverage drops below a lower threshold, then the lattice assumes the hexagonal structure; if it exceeds an upper threshold, then the lattice switches to rectangular.[145]

dx.doi.org/10.1021/cs3005709 | ACS Catal. 2012, 2, 2648−2663

Aside from reconstruction, there are many other phenomena involving complex catalyst dynamics that await fundamental modeling. Catalyst sintering is one[146,147] and mixing of bimetallic catalysts is yet another.[148] Growth, sintering, and coarsening phenomena for 2D and 3D clusters have been investigated by KMC in the context of epitaxial growth.[149] Moreover, the limited number of aforementioned studies has provided insights into the effects of reconstruction on catalytic properties. Yet, a fundamental understanding of the intimate interplay between catalyst dynamics and catalysis necessitates the development of first-principles approaches that would integrate the elementary processes of catalyst dynamics with those of surface reaction. This is a particularly challenging endeavor for several reasons: the elementary events involved in catalyst dynamics are nontrivial to identify and parameterize, since they include many body effects (adsorbates and catalyst atoms) and manifest via the concerted motion of several atoms.[150] Moreover, creating a catalogue of all elementary events of the catalyst dynamics and possible reactions on the emerging sites would dramatically increase bookkeeping requirements in a KMC simulation and require an enormous number of DFT calculations. This hurdle may require a different computational approach, such as molecular dynamics, to cope with multidimensional reaction coordinates coupled with a KMC model. Unfortunately, molecular dynamics is usually too slow unless some acceleration method is employed. Finally, there is a vast range of time scales in which catalyst dynamics takes place, ranging from nanoseconds up to several hours.[151] The challenges of chemical complexity and separation of time scales are further discussed in the next section.

Computational Challenges. Apart from the challenges of incorporating all relevant physical processes into KMC models, first-principles KMC simulation is nontrivial. A number of computational challenges are encountered, namely, the efficient simulation of large chemical reaction networks involving several strongly interacting adsorbates, the efficient treatment of time scales spanning orders of magnitude, and the systematic assessment of the variability of results with respect to perturbations in the input parameters. Because of these challenges, short-cuts are often employed whose impact on the predictions has been hard to evaluate. Below we outline some of these challenges and directions for future research.

Chemical Complexity Arising from Large Reaction Networks. Simulating realistic chemistries necessitates taking into account a large number of elementary events, representing all possible adsorption, desorption, diffusion and surface (Langmuir−Hinshelwood or Eley−Rideal) reactions. This chemical complexity implies a large number of computationally intensive DFT calculations to obtain the kinetic parameters of all individual elementary steps, that is, creating a kinetic database is impractical for large chemistries even for mean-field models. Including variants of a reaction, in which the same species appear in different binding configurations (for instance at step or terrace sites), further exacerbates this problem. As an example, a KMC model of the water-gas shift reaction on Pt(211) contains 152 elementary steps, whereas a mean-field model of the same chemistry on Pt(111) would have only 34 elementary steps.[41]

Resolving the problem pertinent to constructing a huge kinetic database calls for the development of accurate semiempirical methods. We have proposed to estimate parameters first by employing linear free energy (Brønsted-Evans-Polanyi (BEP)) relations or BOC models instead of calculating all possible elementary steps using DFT. Then, hierarchical refinement can be used to obtain accurate values for the crucial parameters via DFT. For a review of these methods the reader is referred to Salciccioli et al.[152] Alternatively, self-learning KMC techniques may be used to interface the KMC and DFT codes and calculate only the relevant configurations that may result in a reaction event.[153,154]

At each step of a KMC simulation where an event is executed, the lattice state and the list of all processes are updated. This update necessitates scanning for the new possible adsorption, desorption, diffusion, and reaction events that can take place. This scanning can become time-consuming for large reaction networks. In particular, the simulation time (normalized with the number of events), scales linearly with the number of elementary steps of the reaction network for the chemistries of Table 1 (Figure 6a). When energetic interactions are included in a simulation, the overhead can become tremendous as demonstrated in Figure 6b and Table 2, since one has to also scan for the energetic interaction patterns included in the cluster expansion of the Hamiltonian. Efficient search and update algorithms can be used to reduce computational cost,[17] so that only relevant reactions are considered when the lattice is updated. Parallelization is another option. For example, since different possible reaction patterns can be scanned independently, one may employ more than one processor during the scan, thereby speeding up the procedure.

Table 1. Elementary Events and Rate Parameters of the Chemistries Simulated in Figure 6[a]

	reversible step	k_{fwd} (s^{-1})	k_{rev} (s^{-1})
	Table 1a: CO Oxidation		
1	$CO_{(g)} + * \leftrightarrow CO*$	5.78×10^5	1.65×10^3
2	$O_{2(g)} + 2\,* \leftrightarrow 2\,O*$	1.62×10^5	2.33×10^{11}
3	$CO* + O* \leftrightarrow CO_{2(g)} + 2\,*$	1.71×10^2	0.00
	Table 1b: NH_3 Decomposition		
1	$H_{2(g)} + 2\,* \leftrightarrow 2\,H*$	0.00	3.68×10^5
2	$N_{2(g)} + 2\,* \leftrightarrow 2\,N*$	0.00	1.41×10^1
3	$NH_{3(g)} + * \leftrightarrow NH_3*$	3.94×10^4	9.00×10^6
4	$N* + H* \leftrightarrow NH* + *$	0.18	1.15×10^{10}
5	$NH* + H* \leftrightarrow NH_2* + *$	4.45×10^5	4.27×10^6
6	$NH_2* + H* \leftrightarrow NH_3* + *$	1.87×10^6	1.05×10^7
	Table 1c: Water-Gas Shift		
1	$CO_{(g)} + * \leftrightarrow CO*$	1.70×10^4	1.60×10^4
2	$O_{2(g)} + 2\,* \leftrightarrow 2\,O*$	0.00	1.00×10^{-8}
3	$H_{2(g)} + 2\,* \leftrightarrow 2\,H*$	0.00	5.14×10^2
4	$CO_{2(g)} + 2\,* \leftrightarrow CO* + O*$	0.00	7.61
5	$H_2O_{(g)} + * \leftrightarrow H_2O*$	6.48×10^5	5.09×10^9
6	$H_2O* + * \leftrightarrow OH* + H*$	1.26×10^6	2.11×10^9
7	$OH* + * \leftrightarrow O* + H*$	2.57×10^5	9.76
8	$2\,OH* \leftrightarrow O* + H_2O*$	3.09×10^{11}	6.96×10^3
9	$CO* + OH* \leftrightarrow COOH* + *$	6.65×10^6	3.12×10^3
10	$COOH* \leftrightarrow H* + CO_{2(g)}$	9.32×10^7	0.00

[a]Note that each reversible step counts as two elementary steps.

Accurate Adlayer Energetic Models. Most KMC simulations employ the nearly zero coverage-limit kinetic parameters from DFT and may include lateral interactions for a couple of species. Accounting for accurate lateral interactions is necessary, in view of the fact that they can have a marked effect on reaction barriers and thus rate constants, as portrayed in Figure 7 and discussed later in this section. Constructing accurate models of the adlayer energetics for multicomponent systems is however a major undertaking. Specifically, the ECIs of a cluster expansion Hamiltonian have to be estimated via fitting the energies

dx.doi.org/10.1021/cs3005709 | ACS Catal. 2012, 2, 2648−2663

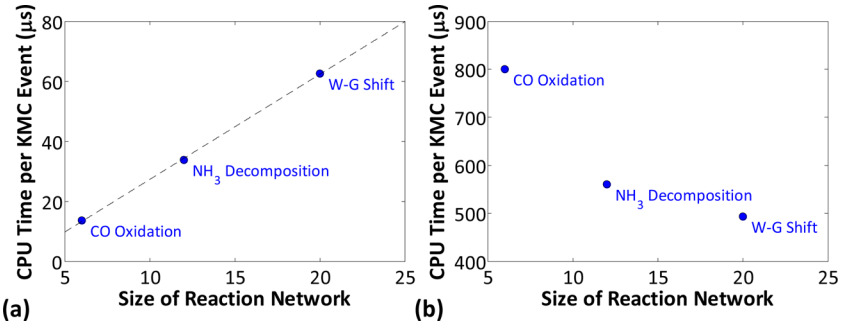

Figure 6. (a) CPU time per kinetic Monte Carlo event for simple chemistries: CO oxidation (6 elementary steps), NH_3 decomposition (12 elementary steps) and water-gas shift (20 elementary steps). The CPU time scales linearly with the number of elementary steps in the reaction network. The reactions included in each chemistry are listed in Table 1. (b) As in panel (a) but with the following pairwise additive energetic interactions included in the models: for CO oxidation: CO−CO, CO−O, O−O; for NH_3 decomposition: N−N, H−H; and for water-gas shift: CO−CO. The computational overhead increases rapidly with the number of interactions. Table 2 presents the CPU times plotted in this figure.

Table 2. CPU Times per KMC Event (in μs) for Three Different Chemistries When Energetic Interactions Are Absent from or Included in the Models

	CO oxidation	NH_3 decomposition	water-gas shift
no energetic interactions	13.5	33.8	62.5
with energetic interactions	799.5	559.8	492.7

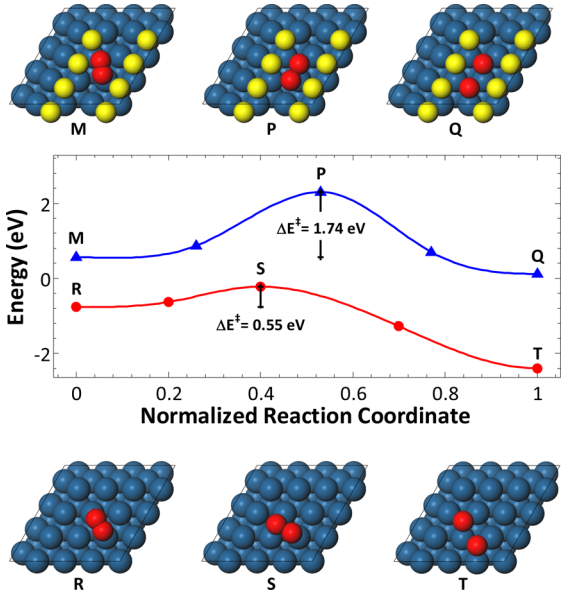

Figure 7. Effect of lateral interactions on the activation barrier for the O_2 dissociation reaction on Pt(111).[160] In the absence of neighboring O adatoms, the barrier is 0.55 eV (path RST). For a 1/2 monolayer coverage, the barrier becomes 1.74 eV (path MPQ), an increase of more than 3-fold. Redrawn from ref 160 (Getman et al.).

obtained by DFT calculations (see section "Cluster-Expansion Hamiltonians"). Thus, one needs to calculate the energy of a number of distinct lattice configurations, which must be no less than the number of clusters included in the expansion. For illustration purposes, consider fitting an Ising-type Hamiltonian that includes short and long-ranged pairwise interactions for several surface species on a regular lattice:

$$\mathrm{H}(\boldsymbol{\sigma}) = H_0 + \sum_{k=1}^{N_S}\sum_{i=1}^{N_L} \beta_k^{s(i)}\cdot\sigma_{i,k} + \frac{1}{2}\cdot\sum_{k=1}^{N_S}\sum_{m=1}^{N_S}\sum_{i=1}^{N_L}\sum_{\substack{j=1\\ i\neq j}}^{N_L} J_{k,m}^{s(i),s(j)}\cdot\sigma_{i,k}\cdot\sigma_{j,m} \quad (4)$$

where N_S is the number of surface species, N_L the number of lattice sites, and $\sigma_{i,k}$ the occupancy, which is equal to 1 if site i is occupied by species k, and 0 otherwise (according to the lattice-gas convention). Moreover, $s(i)$ denotes the site type for site i and ranges from 1 to N_T, the number of different site types. The ECIs in this case include H_0, which is a single constant; $\beta_k^{s(i)}$, which is the binding energy of species k to site $s(i)$, and $J_{k,m}^{s(i),s(j)}$ which is the pair interaction energy for species k and m bound at sites $s(i)$ and $s(j)$. Assuming that the pair interaction energy depends only on the distance of the two sites and that the model takes into account n such distinct distances (for instance fit up to the n-th nearest neighbor), then the number of parameters to be determined is equal to

$$1 + N_S\cdot N_T + \frac{1}{2}\cdot n\cdot N_S\cdot N_T\cdot(N_S\cdot N_T - 1) \quad (5)$$

where N_T denotes the number of different site types. The factor 1/2 comes from the symmetry in the pair interaction, in particular $J_{k,m}^{s(i),s(j)} = J_{m,k}^{s(j),s(i)}$ and prevents double-counting of pairs. Equation 5 shows that the number of parameters increases rapidly for complex reaction mechanisms. For instance, in ethylene glycol decomposition chemistry, N_S = 30. Assuming a single site type and up to second nearest neighbor interactions (n = 2), one would have to fit 901 parameters. In practice, one needs even more DFT calculations than the number of parameters, to have a sense of the fitting error. Constructing a multispecies cluster expansion Hamiltonian can thus become impractical, especially if one needs to include long-ranged interactions or many-body terms.

Overcoming this problem could potentially be achieved by employing a smart "training" procedure, rather than a priori fitting for the ECIs of all possible clusters. Presumably, the most important terms in the Hamiltonian are one- and two-body terms, which will have to be included first. Then, by using a refinement procedure, based on genetic algorithms[155,156] or neural networks coupled with a novelty sampling,[157,158] one could include only the important configurations that affect the

dx.doi.org/10.1021/cs3005709 | ACS Catal. 2012, 2, 2648−2663

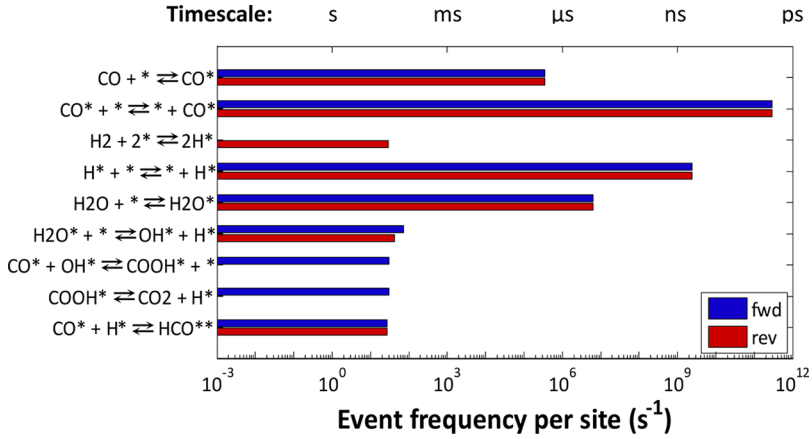

Figure 8. Time scales for the adsorption, desorption, surface diffusion, and reaction events for the water-gas shift reaction on Pt(111)[40] under the following conditions: T = 650 K, P = 1 bar; gas molar fractions: y_{CO} = 0.05, y_{H2O} 0.10, y_{H2} = y_{CO2} = 0.00.

energetics, thereby improving the accuracy of the Hamiltonian, on an "as needed" basis.

Optimal selection of lattice configurations whose energy is to be computed using first principles calculations and then used in fitting is also important.[159] In a hierarchical refinement scheme, an initial set of lattice configurations is supplied to a DFT code. The energies computed therefrom are used to construct an approximate cluster expansion, which is used to generate configurations close to the system's ground-state. If these configurations have already been included in the expansion, convergence has been achieved. Otherwise, the energies of these configurations are computed via DFT, a new fitting of the ECIs is performed, and the procedure is repeated until convergence. Seko et al.[159] argue that while this procedure is adequate for parametrizing the energy in the vicinity of a ground state, it will result in significant error for systems with large configurational entropies, for instance in order−disorder transition phenomena. In such cases, configurations away from the ground state are frequently sampled, and thus have a significant contribution to the system's free energy. Seko et al.[159] propose a procedure that overcomes this limitation and greatly improves the accuracy of the expansion.

Tackling KMC simulation of surface kinetics involving complicated energetics models would necessitate the development of algorithms for efficient pattern search. Sophisticated bookkeeping procedures would also be needed to avoid rescanning the same configurations (patterns). Parallelization techniques would also be invaluable, since identification of different patterns can be done independently, and the summation of the energetic contributions thereof would only incur a minor communication overhead.

The discussion of the cluster expansions has so far been limited to the thermodynamics of the adlayer. The reaction barrier obtained from DFT pertains to the zero (or, in practice, low) coverage-limit and has to be corrected to include finite coverage effects. These effects may be significant, for instance in the case of O_2 dissociation on Pt(111), the barrier at the zero coverage limit is around 1/2 eV, and increases more than 3-fold for a half-monolayer coverage (Figure 7).[160] To account for such effects, in principle, one can construct a cluster expansion for the interactions between a TS and the various adsorbates. Such an energetic model would constitute an accurate description of the barrier of a reaction as a function of the local environment and ensure thermodynamic consistency of the entire reaction mechanism. This, however, would be a daunting task, and in practice, one resorts to simpler approaches such as the development of linear scaling relations that correlate the reaction barrier to the initial and/or final state energies.[64] The latter energies can relatively easily be computed from the cluster expansion of the Hamiltonian for the adlayer energetics. The impact of this approximation on the accuracy of the overall framework is currently unclear. Some examples of error quantification of at least simple systems will be very desirable. Overall, development of methods that accurately and efficiently (i.e., with minimal DFT calculations) parameterize the reaction rate constants as a function of the local configuration of adsorbates is a critical methodological step of the ab initio KMC method.

Time Scale Separation. Disparity in time scales of various processes (known also as stiffness) is commonplace in chemical kinetics. For instance, diffusion events typically occur on the nano- to picosecond scale, adsorption/desorption events on the microsecond scale, and reactions may exhibit even slower dynamics (for an example, see Figure 8).[128] While solvers exist for stiff deterministic problems, this is not the case in KMC simulation. As a result, a KMC simulation would spend most of the computational time executing uninteresting diffusional hops, rather than the reaction events which are of importance in estimating catalytic activity. Previous studies have either neglected fast processes, for example, diffusion, or employed equilibration of the lattice to overcome the problem of fast diffusion.[12,161] While this is certainly valid for simple systems, it is not obvious that diffusion is always fast: in particular, hopping from a low energy site, where the binding is strong (e.g., a step site), to a high energy site, where the binding is weak (e.g., a terrace site), could be associated with a large barrier. Such a hopping process may be slow and thus crucial in shaping the dynamics. Aside from surface diffusion, in large reaction networks, a subset of the chemistry is fast (e.g., adsorption/desorption or (de)hydrogenation) and partially equilibrated whereas the rest is not. Thus, the problem of time scale separation is more often than not found in many physical processes. Reaction barriers or even reaction rate constants are inadequate to establish time scale separation; rather, reaction rates are needed, which of course require solving the entire problem.

Dealing with time scale separation efficiently would still involve decomposing fast and slow modes and treating the fast

dx.doi.org/10.1021/cs3005709 | ACS Catal. 2012, 2, 2648−2663

ones as quasi equilibrated. The mathematical foundations handling stiffness were introduced a while back.[17,162−167] Mathematical and computational analysis, using singular perturbation, has shown that the error incurred in such a treatment is on the order of the ratio of the slow versus fast rates.[168] Despite significant progress for prototype models, a computational scheme that detects the fast processes automatically (on-the-fly), performs the decomposition, and updates the various processes dynamically is currently lacking. This dynamic update is challenging but important, since the temporal evolution of surface coverages can result in large changes in the rates of certain elementary events, making it necessary to re-evaluate which modes are treated as fast.

Sensitivity Analysis and Uncertainty Quantification. A major task in first-principles KMC simulation is to carry out a sensitivity analysis to identify the rate controlling step according to the DRC method and understand the important chemistry.[169] Performing sensitivity analysis for large reaction networks efficiently is nontrivial, given the stochastic nature of the output and the computational expense of KMC simulation. Utilizing a brute-force finite difference scheme, where each rate constant is varied and the simulation repeated ends up being computationally intractable. State-of-the-art methods that have already been used successfully in the sensitivity analysis of biochemical reaction networks could also be adapted in surface kinetics KMC simulation. For instance the common random number (CRN) and the common reaction path (CRP) methods reduce the computational effort required to compute the sensitivity coefficients.[170] Other computational schemes based on likelihood ratio gradient estimation could also be used in this context.[171] These methods are intended for local sensitivity analysis. Alternatively, one can perform global sensitivity analysis using polynomial chaos expansions[172,173] or polynomial dimensional decompositions.[174] Global sensitivity methods offer advantages: they evaluate the effect of collective uncertainty and are not restricted to small perturbations in the input parameters (contrary to the finite difference schemes).

Aside from sensitivity analysis, uncertainty quantification (UQ) is highly desirable to assess the robustness of results, given that small errors in the activation energy can result in large errors in the calculated rate. As an example, an error of 3 kcal/mol (0.13 eV) in the activation energy (which is on the low end of the expected DFT error),[175] will result in a relative error of 20 in the rate at 500 K. The situation becomes much worse at lower temperatures. UQ studies will be useful in potentially rationalizing the deviations between experiments and KMC simulation results observed in a number of studies, most notably by Sendner et al.[119] (see section on Partial Oxidation of Methanol) or the qualitative changes of the underlying physics if different parameter sets are being used[70] (see section on CO Oxidation). To the best of our knowledge, no such studies have been conducted.

SUMMARY AND OUTLOOK

The coupling of DFT calculations with kinetic Monte Carlo (KMC) simulations provides a powerful multiscale modeling framework, termed first principles or ab initio KMC method, that can be used to elucidate the chemical processes on catalytic surfaces with unprecedented spatiotemporal detail. The basic idea behind this framework is to simulate a sequence of adsorption, desorption, diffusion, and reaction events, the rates of occurrence of which are calculated through first-principles density functional theory and TST approximations. A strength of the method is that it can naturally account for spatial inhomogeneities of the catalyst and adsorbates.

This approach has been successfully applied to a number of chemistries reviewed herein. These studies have shed light on the effect of surface structure or promoters on activity, identification of the rate determining step, or experimentally obtained thermal desorption spectra. Several of these effects can be captured, at least qualitatively, by mean-field microkinetic models. The impact of KMC simulation will mainly be manifested in problems incorporating spatial effects where multiple active sites are involved and the activity and selectivity arise from nonlinear coupling among these sites. Examples include the dependence of the structure sensitivity of a reaction on nanoparticle size and shape, promoters, whose specific location may be important, multifunctional materials (e.g., Lewis and Brønsted acid sites or metal and Brønsted acid sites), and support effects due to parts of the chemistry occurring on the support, the metal sites and interfacial support/metal sites. The ongoing efforts to incorporate more detailed physics and chemistry in these simulations in conjunction with the never-ending pursuit of more efficient methodologies is bound to improve the predictive power of first-principles KMC, making it a quantitative tool for mechanism understanding and eventually in silico catalyst discovery and optimization.

ASSOCIATED CONTENT

Supporting Information

Further details on the rate expressions for elementary events. This material is available free of charge via the Internet at http://pubs.acs.org.

AUTHOR INFORMATION

Corresponding Author

*E-mail: vlachos@udel.edu. Phone: +1-302-831-2830.

Notes

The authors declare no competing financial interest.

ACKNOWLEDGMENTS

The research was partially supported by Grant DE-FG02-05ER25702 from the Department of Energy.

REFERENCES

(1) Jacobsen, C. J. H.; Dahl, S.; Clausen, B. S.; Bahn, S.; Logadottir, A.; Nørskov, J. K. *J. Am. Chem. Soc.* **2001**, *123* (34), 8404.
(2) Greeley, J.; Jaramillo, T. F.; Bonde, J.; Chorkendorff, I. B.; Nørskov, J. K. *Nat. Mater.* **2006**, *5* (11), 909.
(3) Greeley, J.; Mavrikakis, M. *Nat. Mater.* **2004**, *3* (11), 810.
(4) Hansgen, D. A.; Vlachos, D. G.; Chen, J. G. G. *Nat. Chem.* **2010**, *2* (6), 484.
(5) Jiang, T.; Mowbray, D. J.; Dobrin, S.; Falsig, H.; Hvolbæk, B.; Bligaard, T.; Nørskov, J. K. *J. Phys. Chem. C* **2009**, *113* (24), 10548.
(6) Bligaard, T.; Nørskov, J. K.; Dahl, S.; Matthiesen, J.; Christensen, C. H.; Sehested, J. *J. Catal.* **2004**, *224* (1), 206.
(7) Falsig, H.; Hvolbæk, B.; Kristensen, I. S.; Jiang, T.; Bligaard, T.; Christensen, C. H.; Nørskov, J. K. *Angew. Chem., Int. Ed.* **2008**, *47* (26), 4835.
(8) Dumesic, J. A.; Rudd, D. F.; Aparicio, L. M.; Rekoske, J. E. *The Microkinetics of Heterogeneous Catalysis*; American Chemical Society: Washington, DC, 1993.
(9) Mhadeshwar, A. B.; Vlachos, D. G. *J. Phys. Chem. B* **2004**, *108* (39), 15246.
(10) Grabow, L. C.; Gokhale, A. A.; Evans, S. T.; Dumesic, J. A.; Mavrikakis, M. *J. Phys. Chem. C* **2008**, *112* (12), 4608.
(11) Neurock, M.; Hansen, E. W. *Comput. Chem. Eng.* **1998**, *22*, S1045.

(12) Hansen, E. W.; Neurock, M. *Chem. Eng. Sci.* **1999**, *54* (15−16), 3411.
(13) Reuter, K.; Frenkel, D.; Scheffler, M. *Phys. Rev. Lett.* **2004**, *93* (11), 116105.
(14) Reuter, K. First-Principles Kinetic Monte Carlo Simulations for Heterogeneous Catalysis: Concepts, Status and Frontiers. In *Modeling Heterogeneous Catalytic Reactions: From the Molecular Process to the Technical System*; Deutschmann, O., Ed.; Wiley-VCH: Weinheim, Germany, 2010.
(15) Bortz, A. B.; Kalos, M. H.; Lebowitz, J. L. *J. Comput. Phys.* **1975**, *17* (1), 10.
(16) Hänggi, P.; Talkner, P.; Borkovec, M. *Rev. Mod. Phys.* **1990**, *62*, 251.
(17) Chatterjee, A.; Vlachos, D. G. *J. Comput.-Aided Mater. Des.* **2007**, *14* (2), 253.
(18) Kang, H. C.; Weinberg, W. H. *Chem. Rev.* **1995**, *95* (3), 667.
(19) Ziff, R. M.; Gulari, E.; Barshad, Y. *Phys. Rev. Lett.* **1986**, *56* (24), 2553.
(20) Vlachos, D. G.; Schmidt, L. D.; Aris, R. *Surf. Sci.* **1991**, *249* (1−3), 248.
(21) Zhdanov, V. P.; Kasemo, B. *Surf. Sci. Rep.* **1994**, *20* (3), 113.
(22) Lukkien, J. J.; Segers, J. P. L.; Hilbers, P. A. J.; Gelten, R. J.; Jansen, A. P. J. *Phys. Rev. E* **1998**, *58* (2), 2598.
(23) Dooling, D. J.; Broadbelt, L. J. *Ind. Eng. Chem. Res.* **2001**, *40* (2), 522.
(24) Kohn, W. *Rev. Mod. Phys.* **1999**, *71* (5), 1253.
(25) Hohenberg, P.; Kohn, W. *Phys. Rev. B* **1964**, *136* (3), B864.
(26) Kohn, W.; Sham, L. J. *Phys. Rev.* **1965**, *140* (4), A1133.
(27) Burke, K. *The ABC of DFT*; Department of Chemistry, University of California: Irvine, CA, 2003, http://dft.uci.edu/sites/default/files/g1.pdf.
(28) Martin, R. M. *Electronic Structure: Basic Theory and Practical Methods*; Cambridge University Press: Cambridge, U.K., 2004.
(29) Sabbe, M. K.; Reyniers, M.-F.; Reuter, K. *Catal. Sci. Technol.* **2012**, *2* (10), 2010.
(30) Pechukas, P. Statistical Approximations in Collision Theory. In *Dynamics of Molecular Collisions. Part B*; Miller, W. H., Ed.; Plenum Press: New York, 1976.
(31) Henkelman, G.; G. Jóhannesson, H. Jónsson Methods for Finding Saddle Points and Minimum Energy Paths. In *Progress on Theoretical Chemistry and Physics*; Schwartz, S. D., Ed.; Kluwer Academic Publishers: Dordrecht, The Netherlands, 2000; p 269.
(32) Henkelman, G.; Jónsson, H. *J. Chem. Phys.* **1999**, *111* (15), 7010.
(33) Henkelman, G.; Uberuaga, B. P.; Jónsson, H. *J. Chem. Phys.* **2000**, *113* (22), 9901.
(34) Jónsson, H.; Mills, G.; Jacobsen, K. W. Nudged elastic band method for finding minimum energy paths of transitions. In *Classical and Quantum Dynamics in Condensed Phase Simulations*; Berne, B. J., Ciccotti, G., Coker, D. F., Eds.; World Scientific: Singapore, 1998; p 385.
(35) Hansen, E.; Neurock, M. *Surf. Sci.* **1999**, *441* (2−3), 410.
(36) Vlachos, D. G. *Adv. Chem. Eng.* **2005**, *30*, 1.
(37) Reuter, K.; Scheffler, M. *Phys. Rev. B* **2006**, *73* (4), 045433.
(38) Jansen, A. P. J.; Lukkien, J. J. *Catal. Today* **1999**, *53* (2), 259.
(39) CARLOS *Project: a general purpose program for the simulation of chemical reactions taking place at crystal surfaces*. Available from: http://carlos.win.tue.nl/
(40) Stamatakis, M.; Vlachos, D. G. *J. Chem. Phys.* **2011**, *134* (21), 214115.
(41) Stamatakis, M.; Chen, Y.; Vlachos, D. G. *J. Phys. Chem. C* **2011**, *115* (50), 24750.
(42) Stamatakis, M.; Christiansen, M.; Vlachos, D. G.; Mpourmpakis, G. *Nano Lett.* **2012**, *12* (7), 3621.
(43) Schmidt, D. J.; Chen, W.; Wolverton, C.; Schneider, W. F. *J. Chem. Theory Comput.* **2012**, *8* (1), 264.
(44) Miller, S. D.; Kitchin, J. R. *Mol. Simul.* **2009**, *35* (10−11), 920.
(45) Zhang, Y. S.; Blum, V.; Reuter, K. *Phys. Rev. B* **2007**, *75* (23), 235406.
(46) Liu, D. J.; Evans, J. W. *ChemPhysChem* **2010**, *11* (10), 2174.
(47) Maestri, M.; Reuter, K. *Angew. Chem., Int. Ed.* **2011**, *50* (5), 1194.
(48) Sanchez, J. M.; Ducastelle, F.; Gratias, D. *Phys. A* **1984**, *128* (1−2), 334.
(49) Tang, H. R.; Van der Ven, A.; Trout, B. L. *Phys. Rev. B* **2004**, *70* (4), 045420.
(50) Han, B. C.; Van der Ven, A.; Ceder, G.; Hwang, B.-J. *Phys. Rev. B* **2005**, *72* (20), 205409.
(51) Stampfl, C. *Catal. Today* **2005**, *105* (1), 17.
(52) Piccinin, S.; Stampfl, C. *Phys. Rev. B* **2010**, *81* (15), 155427.
(53) Lazo, C.; Keil, F. J. *Phys. Rev. B* **2009**, *79* (24), 245418.
(54) Drautz, R.; Singer, R.; Fähnle, M. *Phys. Rev. B* **2003**, *67* (3), 035418.
(55) Drautz, R.; Diaz-Ortiz, A. *Phys. Rev. B* **2006**, *73* (22), 224207.
(56) Lerch, D.; Wieckhorst, O.; Hammer, L.; Heinz, K.; Müller, S. *Phys. Rev. B* **2008**, *78* (12), 121405.
(57) van de Walle, A.; Asta, M.; Ceder, G. *Calphad* **2002**, *26* (4), 539.
(58) van de Walle, A.; Ceder, G. *J. Phase Equilib.* **2002**, *23* (4), 348.
(59) Lerch, D.; Wieckhorst, O.; Hart, G. L. W.; Forcade, R. W.; Müller, S. *Modell. Simul. Mater. Sci. Eng.* **2009**, *17* (5), 055003.
(60) Stampfl, C.; Kreuzer, H. J.; Payne, S. H.; Pfnür, H.; Scheffler, M. *Phys. Rev. Lett.* **1999**, *83* (15), 2993.
(61) Franz, T.; Mittendorfer, F. *J. Chem. Phys.* **2010**, *132* (19), 194701.
(62) McEwen, J. S.; Eichler, A. *J. Chem. Phys.* **2007**, *126* (9), 094701.
(63) Jansen, A. P. J.; Offermans, W. K. *Comput. Sci. Appl. - ICCSA 2005* **2005**, *3480*, 251.
(64) Wu, C.; Schmidt, D. J.; Wolverton, C.; Schneider, W. F. *J. Catal.* **2012**, *286*, 88.
(65) Ertl, G. *Angew. Chem., Int. Ed.* **2008**, *47* (19), 3524.
(66) Temel, B.; Meskine, H.; Reuter, K.; Scheffler, M.; Metiu, H. *J. Chem. Phys.* **2007**, *126* (20), 204711.
(67) Rieger, M.; Rogal, J.; Reuter, K. *Phys. Rev. Lett.* **2008**, *100* (1), 016105.
(68) Meskine, H.; Matera, S.; Scheffler, M.; Reuter, K.; Metiu, H. *Surf. Sci.* **2009**, *603* (10−12), 1724.
(69) Matera, S.; Meskine, H.; Reuter, K. *J. Chem. Phys.* **2011**, *134* (6), 064713.
(70) Hess, F.; Farkas, A.; Seitsonen, A. P.; Over, H. *J. Comput. Chem.* **2012**, *33* (7), 757.
(71) Kiejna, A.; Kresse, G.; Rogal, J.; De Sarkar, A.; Reuter, K.; Scheffler, M. *Phys. Rev. B* **2006**, *73* (3), 035404.
(72) Seitsonen, A. P.; Over, H. *Surf. Sci.* **2009**, *603* (10−12), 1717.
(73) Ulissi, Z.; Prasad, V.; Vlachos, D. G. *J. Catal.* **2011**, *281* (2), 339.
(74) Nagasaka, M.; Kondoh, H.; Nakai, I.; Ohta, T. *J. Chem. Phys.* **2007**, *126* (4), 044704.
(75) Rogal, J.; Reuter, K.; Scheffler, M. *Phys. Rev. B* **2008**, *77* (15), 155410.
(76) Liu, D. J.; Evans, J. W. *Surf. Sci.* **2009**, *603* (10−12), 1706.
(77) Petrova, N. V.; Yakovkin, I. N. *Surf. Sci.* **2005**, *578* (1−3), 162.
(78) Völkening, S.; Wintterlin, J. *J. Chem. Phys.* **2001**, *114* (14), 6382.
(79) Cortés, J.; Valencia, E. *Phys. Rev. E* **2005**, *71* (4), 046136.
(80) Cortés, J.; Valencia, E. *J. Phys. Chem. B* **2006**, *110* (15), 7887.
(81) Cortés, J.; Valencia, E. *Bull. Chem. Soc. Jpn.* **2008**, *81* (10), 1267.
(82) Ahmad, W.; Baloch, M. K. *Appl. Surf. Sci.* **2007**, *253* (20), 8447.
(83) Olsson, L.; Zhdanov, V. P.; Kasemo, B. *Surf. Sci.* **2003**, *529* (3), 338.
(84) Rafti, M.; Vicente, J. L. *Phys. Rev. E* **2007**, *75* (6), 061121.
(85) Alas, S. J.; Vicente, L. *Surf. Sci.* **2010**, *604* (11−12), 957.
(86) Alvarez-Falcon, L.; Vicente, L. *Int. J. Quantum Chem.* **2012**, *112* (7), 1803.
(87) Fink, T.; Dath, J. P.; Imbihl, R.; Ertl, G. *J. Chem. Phys.* **1991**, *95* (3), 2109.
(88) Fink, T.; Dath, J. P.; Imbihl, R.; Ertl, G. *Surf. Sci.* **1991**, *251*, 985.
(89) Khrustova, N.; Veser, G.; Mikhailov, A.; Imbihl, R. *Phys. Rev. Lett.* **1995**, *75* (19), 3564.
(90) Irurzun, I. M.; Mola, E. E.; Imbihl, R. *Chem. Phys.* **2006**, *323* (2−3), 295.
(91) Irurzun, I. M.; Mola, E. E.; Imbihl, R. *J. Phys. Chem. A* **2007**, *111* (17), 3313.
(92) Vantol, M. F. H.; Siera, J.; Cobden, P. D.; Nieuwenhuys, B. E. *Surf. Sci.* **1992**, *274* (1), 63.

(93) Alas, S. J.; Rojas, F.; Kornhauser, I.; Zgrablich, G. *J. Mol. Catal. A: Chem.* **2006**, *244* (1−2), 183.
(94) Alas, S. J.; Zgrablich, G. *J. Phys. Chem. B* **2006**, *110* (19), 9499.
(95) Tammaro, M.; Evans, J. W. *J. Chem. Phys.* **1998**, *108* (18), 7795.
(96) Zhdanov, V. P. *J. Chem. Phys.* **1999**, *110* (17), 8748.
(97) Zhdanov, V. P. *Catal. Lett.* **2004**, *93* (3−4), 135.
(98) Kortlüke, O.; Kuzovkov, V. N.; von Niessen, W. *Phys. Rev. Lett.* **1998**, *81* (10), 2164.
(99) Zhdanov, V. P. *Catal. Lett.* **2002**, *84* (3−4), 147.
(100) Mei, D. H.; Du, J. C.; Neurock, M. *Ind. Eng. Chem. Res.* **2010**, *49* (21), 10364.
(101) van Bavel, A. P.; Hermse, C. G. M.; Hopstaken, M. J. P.; Jansen, A. P. J.; Lukkien, J. J.; Hilbers, P. A. J.; Niemantsverdriet, J. W. *Phys. Chem. Chem. Phys.* **2004**, *6* (8), 1830.
(102) Duca, D.; Botár, L.; Vidóczy, T. *J. Catal.* **1996**, *162* (2), 260.
(103) Hansen, E. W.; Neurock, M. *J. Catal.* **2000**, *196* (2), 241.
(104) Mei, D. H.; Hansen, E. W.; Neurock, M. *J. Phys. Chem. B* **2003**, *107* (3), 798.
(105) Neurock, M.; Mei, D. H. *Top. Catal.* **2002**, *20* (1−4), 5.
(106) Mei, D.; Sheth, P. A.; Neurock, M.; Smith, C. M. *J. Catal.* **2006**, *242* (1), 1.
(107) Mei, D. H.; Neurock, M.; Smith, C. M. *J. Catal.* **2009**, *268* (2), 181.
(108) Aleksandrov, H. A.; Moskaleva, L. V.; Zhao, Z. J.; Basaran, D.; Chen, Z. X.; Mei, D. H.; Rösch, N. *J. Catal.* **2012**, *285* (1), 187.
(109) Christiansen, M. A.; Vlachos, D. G. *Appl. Catal., A* **2012**, *431*−*432*, 18.
(110) Ratnasamy, C.; Wagner, J. P. *Catal. Rev.* **2009**, *51* (3), 325.
(111) Cortright, R. D.; Davda, R. R.; Dumesic, J. A. *Nature* **2002**, *418* (6901), 964.
(112) Li, K.; Fu, Q.; Flytzani-Slephanopoulos, M. *Appl. Catal., B* **2000**, *27* (3), 179.
(113) Wang, G. C.; Jiang, L.; Cai, Z. S.; Pan, Y. M.; Zhao, X. Z.; Huang, W.; Xie, K. C.; Li, Y. W.; Sun, Y. H.; Zhong, B. *J. Phys. Chem. B* **2003**, *107* (2), 557.
(114) Shekhar, M.; Pazmino, J.; Lee, W.; Akatay, M. C.; Stach, E. A.; Miller, J. T.; Delgass, W. N.; Ribeiro, F. H. In *Proceedings of the 2011 Annual Meeting of the American Institute of Chemical Engineers*, Minneapolis, MN, Oct 16−21, 2011.
(115) Hansen, E.; Neurock, M. *J. Phys. Chem. B* **2001**, *105* (38), 9218.
(116) Davis, J. L.; Barteau, M. A. *Langmuir* **1989**, *5* (6), 1299.
(117) Davis, J. L.; Barteau, M. A. *Surf. Sci.* **1991**, *256* (1−2), 50.
(118) Olah, G. A. *Angew. Chem., Int. Ed.* **2005**, *44* (18), 2636.
(119) Sendner, C.; Sakong, S.; Groß, A. *Surf. Sci.* **2006**, *600* (16), 3258.
(120) Wachs, I. E.; Madix, R. J. *J. Catal.* **1978**, *53* (2), 208.
(121) Mei, D. H.; Rousseau, R.; Kathmann, S. M.; Glezakou, V. A.; Engelhard, M. H.; Jiang, W. L.; Wang, C. M.; Gerber, M. A.; White, J. F.; Stevens, D. J. *J. Catal.* **2010**, *271* (2), 325.
(122) Perdew, J. P.; Schmidt, K. *AIP Conference Proceedings - Density Functional Theory and Its Application to Materials* **2001**, *577*, 1.
(123) Schimka, L.; Harl, J.; Stroppa, A.; Gruneis, A.; Marsman, M.; Mittendorfer, F.; Kresse, G. *Nat. Mater.* **2010**, *9* (9), 741.
(124) Gajdoš, M.; Eichler, A.; Hafner, J. *J. Phys.: Condens. Matter* **2004**, *16* (8), 1141.
(125) Feibelman, P. J.; Hammer, B.; Nørskov, J. K.; Wagner, F.; Scheffler, M.; Stumpf, R.; Watwe, R.; Dumesic, J. *J. Phys. Chem. B* **2001**, *105* (18), 4018.
(126) Olsen, R. A.; Philipsen, P. H. T.; Baerends, E. J. *J. Chem. Phys.* **2003**, *119* (8), 4522.
(127) Stroppa, A.; Kresse, G. *New J. Phys.* **2008**, *10*, 063020.
(128) Raimondeau, S.; Vlachos, D. G. *Chem. Eng. J.* **2002**, *90* (1−2), 3.
(129) Vlachos, D. G. *AIChE J.* **1997**, *43* (11), 3031.
(130) Matera, S.; Reuter, K. *Catal. Lett.* **2009**, *133* (1−2), 156.
(131) Matera, S.; Reuter, K. *Phys. Rev. B* **2010**, *82* (8), 085446.
(132) Mei, D. H.; Lin, G. *Catal. Today* **2011**, *165* (1), 56.
(133) Raimondeau, S.; Vlachos, D. G. *Chem. Eng. Sci.* **2003**, *58* (3−6), 657.
(134) Kuramoto, Y. *Prog. Theor. Phys.* **1974**, *52* (2), 711.
(135) Malek-Mansour, M.; Houard, J. *Phys. Lett. A* **1979**, *70* (5−6), 366.
(136) van den Broeck, C. *Phys. Lett. A* **1982**, *90* (3), 119.
(137) Baras, F.; Malek-Mansour, M. Microscopic simulation of chemical instabilities. In *Advances in Chemical Physics*; Prigogine, I., Rice, S. A., Eds.; John Wiley & Sons, Inc: Hoboken, NJ, 1997; Vol. *100*, p 373.
(138) Hattne, J.; Fange, D.; Elf, J. *Bioinformatics* **2005**, *21* (12), 2923.
(139) Bird, G. A. *Commun. Appl. Numer. M* **1988**, *4* (2), 165.
(140) Somorjai, G. A. *Annu. Rev. Phys. Chem.* **1994**, *45*, 721.
(141) Nettesheim, S.; Vonoertzen, A.; Rotermund, H. H.; Ertl, G. *J. Chem. Phys.* **1993**, *98* (12), 9977.
(142) Lele, T. P.; Pletcher, T. D.; Lauterbach, J. *AIChE J.* **2001**, *47* (6), 1418.
(143) Monine, M. I.; Pismen, L. M. *Phys. Rev. E* **2004**, *69* (2), 021606.
(144) Monine, M. I.; Pismen, L. M.; Imbihl, R. *J. Chem. Phys.* **2004**, *121* (22), 11332.
(145) Noussiou, V. K.; Provata, A. *Surf. Sci.* **2007**, *601* (14), 2941.
(146) Meyer, R.; Ge, Q. F.; Lockemeyer, J.; Yeates, R.; Lemanski, M.; Reinalda, D.; Neurock, M. *Surf. Sci.* **2007**, *601* (1), 134.
(147) Meyer, R.; Lockemeyer, J.; YeateS, R.; Lemanski, M.; Reinalda, D.; Neurock, M. *Chem. Phys. Lett.* **2007**, *449* (1−3), 155.
(148) Wang, H.; Stamatakis, M.; Hansgen, D. A.; Caratzoulas, S.; Vlachos, D. G. *J. Chem. Phys.* **2010**, *133*, 224503.
(149) Evans, J. W.; Thiel, P. A.; Bartelt, M. C. *Surf. Sci. Rep.* **2006**, *61* (1−2), 1.
(150) Driver, S. M.; Zhang, T. F.; King, D. A. *Angew. Chem., Int. Ed.* **2007**, *46* (5), 700.
(151) Somorjai, G. A. *Catal. Lett.* **1992**, *12* (1−3), 17.
(152) Salciccioli, M.; Stamatakis, M.; Caratzoulas, S.; Vlachos, D. G. *Chem. Eng. Sci.* **2011**, *66* (19), 4319.
(153) Kara, A.; Trushin, O.; Yildirim, H.; Rahman, T. S. *J. Phys.: Condens. Matter* **2009**, *21* (8), 084213.
(154) Trushin, O.; Karim, A.; Kara, A.; Rahman, T. S. *Phys. Rev. B* **2005**, *72* (11), 115401.
(155) Blum, V.; Hart, G. L. W.; Walorski, M. J.; Zunger, A. *Phys. Rev. B* **2005**, *72* (16), 165113.
(156) Hart, G. L. W.; Blum, V.; Walorski, M. J.; Zunger, A. *Nat. Mater.* **2005**, *4* (5), 391.
(157) Ludwig, J.; Vlachos, D. G. *J. Chem. Phys.* **2007**, *127* (15), 154716.
(158) Ludwig, J.; Vlachos, D. G. *J. Chem. Phys.* **2008**, *128* (15), 154708.
(159) Seko, A.; Koyama, Y.; Tanaka, I. *Phys. Rev. B* **2009**, *80* (16), 165122.
(160) Getman, R. B.; Schneider, W. F.; Smeltz, A. D.; Delgass, W. N.; Ribeiro, F. H. *Phys. Rev. Lett.* **2009**, *102* (7), 076101.
(161) Meng, B.; Weinberg, W. H. *J. Chem. Phys.* **1994**, *100* (7), 5280.
(162) Liu, W. E, D.; Vanden-Eijnden, E. *J. Chem. Phys.* **2005**, *123* (19), 194107.
(163) Liu, W. E, D.; Vanden-Eijnden, E. *J. Comput. Phys.* **2007**, *221* (1), 158.
(164) Salis, H.; Kaznessis, Y. *J. Chem. Phys.* **2005**, *122*, 054103.
(165) Salis, H.; Sotiropoulos, V.; Kaznessis, Y. N. *BMC Bioinf.* **2006**, *7*, 93.
(166) Samant, A.; Ogunnaike, B. A.; Vlachos, D. G. *BMC Bioinf.* **2007**, *8*, 175.
(167) Samant, A.; Vlachos, D. G. *J. Chem. Phys.* **2005**, *123* (14), 144114.
(168) Stamatakis, M.; Vlachos, D. G. *Comput. Chem. Eng.* **2011**, *35* (12), 2602.
(169) Campbell, C. T. *J. Catal.* **2001**, *204* (2), 520.
(170) Rathinam, M.; Sheppard, P. W.; Khammash, M. *J. Chem. Phys.* **2010**, *132* (3), 034103.
(171) McGill, J. A.; Ogunnaike, B. A.; Vlachos, D. G. *J. Comput. Phys.* **2012**, *231* (30), 7170−7186.
(172) Sudret, B. *Reliab. Eng. Syst. Saf.* **2008**, *93* (7), 964.
(173) Xiu, D. *Numerical Methods for Stochastic Computations: A Spectral Method Approach*; Princeton University Press: Princeton, NJ, 2010.
(174) Rahman, S. *Reliab. Eng. Syst. Saf.* **2011**, *96* (7), 825.

(175) Hammer, B.; Hansen, L. B.; Nørskov, J. K. *Phys. Rev. B* **1999**, *59* (11), 7413.

dx.doi.org/10.1021/cs3005709 | *ACS Catal.* 2012, 2, 2648−2663